Inhibition of hepatitis B virus activities by *Rhazya stricta*-derived acacetin and acetyl-β-carboline

MOHAMMAD K. PARVEZ, TAWFEQ A. ALHOWIRINY, MOHAMMED S. AL-DOSARI, MUSARAT AMINA, MD TABISH REHMAN, HANAN M. AL-YOUSEF, ABDULLAH R. ALANZI and MOHAMMED F. ALAJMI

Department of Pharmacognosy, College of Pharmacy, King Saud University, Riyadh 11451, Kingdom of Saudi Arabia

Received January 22, 2023; Accepted April 24, 2023

DOI: 10.3892/etm.2023.12026

Abstract. Hepatitis B virus (HBV) causes acute and chronic liver diseases, leading to cirrhosis and hepatocellular carcinoma. Although direct-acting nucleoside analogs, such as lamivudine (LAM), adefovir and famciclovir, are available, emergence of drug-resistance due to mutations in HBV polymerase (POL) restricts their further use. Alternatively, numerous plant products and compounds isolated from plants have been reported to confer anti-HBV efficacies without any sign of resistance *in vitro* or *in vivo*. As, flavonoids and alkaloids are the most widely reported antivirals, the anti-HBV activities of the flavonoid acacetin (ACT) and the alkaloid acetyl-β-carboline (ABC) from the aerial parts of *Rhazya stricta* were assessed in the present study. Both compounds were isolated from the ethyl acetate fraction of the total methanol extract using column and thin-layer chromatography, and their structures were determined by nuclear magnetic resonance spectroscopy (NMR). Both compounds (at 6.25-50 μg/ml) showed a lack of hepatocytotoxicity in cultured HepG2.2.15 cells. Anti-HBV ELISA [hepatitis B surface antigen (HBsAg) and hepatitis B pre-core-antigen (HBeAg)] on HepG.2.2.15 cells following treatment with selected concentrations (12.5, 25 and 50 μg/ml) of both compounds showed dose- and time-dependent anti-HBV activities. Compared with those in the untreated control at day 5, ACT and ABC (25 μg/ml, each) maximally inhibited HBsAg synthesis by 43.4 and 48.7%, respectively, whilst also maximally inhibiting HBeAg synthesis by 41.2 and 44.2%, respectively, in HepG2.2.15 cells. Comparatively, quercetin and LAM (standards; POL inhibitors) suppressed HBsAg (63.9 and 60.2%, respectively) and HBeAg synthesis (87.1 and 84.3%, respectively) by larger magnitudes. Molecular docking of ACT and ABC structures performed in AutoDock revealed their hydrogen bonding with the drug-sensitive [wild-type (wt)-POL] 'Tyr-Met-Asp-Asp' motif, in addition to the drug-resistant [mutant (mut)-POL] 'Tyr-Ile-Asp-Asp' motif residues of the polymerase binding-pocket, along with other electrostatic interactions. In the wt-POL complex, both compounds showed good interactions with Asp205. In the mut-POL complex, ACT and ABC interacted with Tyr203-Asp205 and Tyr203-Ile204, respectively. In conclusion, to the best of our knowledge, the present study demonstrates anti-HBV efficacies of ACT and ABC *in vitro* for the first time, endorsed by *in silico* data. However, further molecular and pharmacological studies are required to validate their pre-clinical therapeutic potential.

Correspondence to: Professor Mohammad K. Parvez, Department of Pharmacognosy, College of Pharmacy, King Saud University, 23 King Khalid Road, Riyadh 11451, Kingdom of Saudi Arabia
E-mail: mohkhalid@ksu.edu.sa; khalid_parvez@yahoo.com

Key words: hepatitis B virus, anti-hepatitis B virus, *Rhazya stricta*, acacetin, acetyl-β-carboline, cell culture, molecular docking

Introduction

Over the last decade, numerous naturally-occurring or plant products, especially bioactive constituents of different phytochemical classes, have been reported to be viable antiviral agents against several pathogenic viruses, such as human immunodeficiency virus (HIV), herpes simplex virus (HSV), influenza virus (INV), Dengue virus (DENV), Chikungunya virus (CHIKV) and hepatitis C virus (HCV) (1-3). Globally, >300 million individuals have hepatitis B virus (HBV) infection, who may progress into developing chronic diseases, like liver cirrhosis or carcinoma. In addition, some cases may even result in mortality (4). Although efficacious nucleoside analog-based drugs, including the HBV polymerase (POL) inhibitors [such as lamivudine (LAM), adefovir and famciclovir], are available, the emergence of drug-resistance due to mutations in HBV POL due to long-term therapy restricts their further use (5). Alternatively, a range of herbal formulations consisting of isolated phytoconstituents like alkaloids, flavonoids, terpenes and anthraquinones have been widely identified as promising anti-HBV therapeutics with no such resistance *in vitro* or *in vivo* (2,3).

Rhazya stricta Decne (family: Apocynaceae) is a medicinal plant that is distributed in arid South Asian regions, including the Arabian Peninsula (6,7). Traditionally, the leaves, fruits and roots of *R. stricta* have been used to treat various diseases, such as diabetes, fever, sore-throat, helminthiasis, syphilis, rheumatism, inflammation, tooth ache, chest pain, conjunctivitis and constipation (7-9). In addition, pharmacological properties of this plant, such as antioxidant, anticancer, antidiabetic and antihypertensive activities, have also been experimentally

validated using *in vitro* and animal model systems (9). Furthermore, its total ethanolic extracts have been previously shown to exert *in vitro* anti-fungal and anti-bacterial activities (10). Its isolated alkaloids have also been reported to have antitumor, anti-hypertensive and anti-microbial properties in cancer cell lines and microbial culture systems (10). Recently, antiviral activities of the Saudi-grown *R. stricta* leaf extract against INV (11) and severe acute respiratory syndrome coronavirus 2 (12) have been reported. However, to the best of our knowledge, the potential effects of *R. stricta* extracts or phytoconstituents on HBV characteristics remain to be elucidated.

Several phytochemical studies on *R. stricta* have led to the isolation of >100 alkaloids from its roots, flavonoids from the stem, tannins and phenolic compounds from the leaves (7-10,13,14). Among the bioactive flavonoids, rutin, quercetin (QRC), kaempferol, catechin and acacetin (ACT), all of which have already known antiviral activities, have also been identified in *R. stricta* leaves (14,15). However, whilst *in vitro* anti-HBV efficacies of rutin, QRC, kaempferol and catechin have already been reported by previous studies (16-21), the anti-HBV potential of ACT remains elusive. In addition, despite having a unique alkaloid profile (22), β-carboline alkaloids such as 1-acetyl-β-carboline have not been previously reported in *R. stricta*.

Therefore, to the best of our knowledge, the present study reports for the first time the isolation of ABC along with ACT from *R. stricta*, before assessing their anti-HBV activities.

Materials and methods

Plant material and extraction. The fresh aerial parts of *Rhazya stricta* Decne (locally known as Harmal) was collected in June 2021 from the Raudhat AI-Khafs region near Riyadh, Saudi Arabia. The plant material was identified (voucher specimen no. RS-0721) by a phytotaxonomist at the College of Pharmacy, King Saud University (Riyadh, Saudi Arabia). The air-dried powder of the plant material (~3 kg) was extracted with double-distilled water followed by methanol (MeOH) under reflux for 24 h. Both the extracts were filtered through Whatman's paper (no. 1). The water and methanol (MeOH) extracts were obtained by evaporating the solvent in a rotatory vacuum evaporator (Rotavapor R-220; BUCHI Labortechnik AG) at ±40˚C under reduced pressure. The methanol extract (leftover residue) was re-suspended in water and then sequentially fractionated at room temperature (RT) with chloroform ($CHCl_3$) and ethyl acetate (EtOAc). Each fraction was individually filtered and distilled using the rotary vacuum evaporator to furnish the $CHCl_3$-fraction (~102 g) and EtOAc-fraction (~142 g), before being stored at 4˚C until further analysis. All analytical grade solvents were procured from Sigma-Aldrich; Merck KGaA.

Isolation and chemical characterization. The EtOAc-fraction was subjected to column chromatography on a silica gel and eluted with a mixture of solvent (10% MeOH in $CHCl_3$). All eluates (25 drops/min) were pooled together based on their thin-layer chromatography (TLC) patterns under the mobile-phase $CHCl_3$:MeOH (95:5; v/v), producing two spots on the plate. The combined sub-fraction was further subjected to column chromatography and eluted with $CHCl_3$ by gradually varying the percentage (1-5%) of MeOH. The elutes (25 drops/min) showing similar TLC patterns under mobile-phase $CHCl_3$:MeOH (97:3, v/v) were pooled and re-crystallized with MeOH at RT for slow evaporation for 24 h to furnish compound 1 in its purest form (97%). The elutes obtained under mobile-phase $CHCl_3$:MeOH (95:5, v/v) and repeated re-crystallization with MeOH at RT ultimately furnished compound 2 in its purest form. The NMR measurements of the compounds were performed on Bruker Avance 700 spectrometer (Bruker Corporation) with standard pulse sequences operating at 700 and 175 MHz for ^{1}H and ^{13}C NMR, respectively. Therein, tetramethylsilane and DMSO-d6 were used as internal standard and solvent, respectively. EIMS was performed on a Micromass Autospec model (70 eV) spectrometer. HRESIMS spectra were obtained in the positive-ionization mode using an LCT Premier XE Micromass spectrometer (Waters Corporation). Silica gel 60 (230-400 mesh; Merck KGaA) was used for column chromatography, while precoated silica gel plates 60 GF254 (0.25 mm thickness; Merck KGaA) were used for analytical TLC. The chemical structures were determined by comparing their published physical and spectral data (23-25).

Cell cultures and drug. HepG2.2.15, the HBV-reporter cells (derivative of the human hepatoma HepG2 cell line), were a kind gift from Dr Shahid Jameel (Virology Lab. International Centre for Genetic Engineering and Biotechnology, New Delhi, India). The cells were maintained in RPMI-1640 medium (Gibco; Thermo Fisher Scientific, Inc.), supplemented with 10% heat-inactivated bovine serum (Gibco; Thermo Fisher Scientific, Inc.), 1X penicillin-streptomycin mix (HyClone; Cytiva) and 1X sodium pyruvate (HyClone; Cytiva) at 37˚C under 5% CO_2. The HBV POL-inhibitor drug LAM (2 μM; Sigma-Aldrich; Merck KGaA) and the anti-HBV flavonoid QRC (12.5 μg/ml; Sigma-Aldrich; Merck KGaA) were used as standards or positive controls, as described previously (26,27).

Cytotoxicity assay of isolated compounds. Potential cytotoxicity of compounds 1 and 2 isolated from *R. stricta* was tested on HepG.2.2.15 cells, using an MTT assay, to determine their maximally safe concentrations (doses) for subsequent antiviral assays. The test compounds were dissolved in 50 μl dimethyl sulfoxide (DMSO) and re-dissolved in RPMI 1640 to furnish the stock concentration (1 mg/ml), followed by further reconstitution in RPMI to produce the various desired doses. DMSO concentration did not exceed 0.1% even in the maximal dose prepared.

Briefly, HepG2.2.15 cells were seeded ($0.5x10^5$ cells/100 μl/well) in a 96-well culture plate and grown overnight at 37˚C. On the next day, cells were treated (in triplicate) with four different doses (6.25, 12.5, 25 and 50 μg/ml) of compounds 1 and 2, including vehicle or negative control (0.1% DMSO). Following 72 h of incubation at 37˚C, cells were then treated with an MTT reagent (10 μl/well) and incubated for 3.5 h at RT in the dark. Upon the appearance of a purple color, the kit-supplied detergent solution (100 μl/well) was added for cell lysis, followed by 1 h incubation at 37˚C. The optical density (OD; λ=570 nm) was recorded in a microplate reader and analyzed in relation to the negative control, using non-linear

regression (Excel 10.0, Microsoft Corporation) to determine the 50% cytotoxic concentration $(CC)_{50}$ values.

Dose-dependent analysis of hepatitis B surface antigen (HBsAg) inhibition. Compounds 1 and 2 isolated from *R. stricta* at the selected non-cytotoxic concentrations (12.5, 25 and 50 μg/ml) were first assessed to determine their optimal inhibitory dose at day 2 (a single time point). HepG2.2.15 cells were grown in a 96-well plate ($0.5x10^5$/well) overnight at 37˚C. On the next day, the culture media was replenished with fresh media containing three doses (12.5, 25 and 50 μg/ml) of compounds 1 and 2, positive controls (QRC and LAM) or negative (DMSO) controls in triplicates and incubated at 37˚C for 2 days. The culture supernatants of each sample were then collected and quantitatively analyzed for secreted HBsAg using the ELISA kit (Monolisa HBsAg Ultra; cat. no. 72348; Bio-Rad Laboratories, Inc.) according to the protocols of the manufacturer. The OD (λ=460 nm) was recorded using microplate reader and analyzed to determine the inhibition of HBsAg expression (%) in relation to that of the negative control (100% expression). The inhibitory activity (%) of compounds 1 and 2 in comparison to LAM (positive control) was presented.

Time-course analysis of HBsAg inhibition. Following dose-dependent inhibition assay, a time-dependent (days 1, 3 and 5) inhibition (%) analysis of HBsAg at the selected optimal dose (25 μg/ml) of compounds 1 and 2 in relation to the negative control was performed as aforementioned. The inhibitory activity (%) of compounds 1 and 2 in comparison to LAM (positive control) was presented.

Time-course analysis of hepatitis B pre-core-antigen (HBeAg) inhibition. The selected optimal dose (25 μg/ml) of compounds 1 and 2 was subjected to a time-course (days 1, 3 and 5) quantitative analysis of HBeAg secretion in the culture supernatants using ELISA (HBeAg/Anti-HBe Elisa kit; cat. no. KAPG4BNE3; DiaSource ImmunoAssays S.A.) according to the manufacturer's instructions. The OD (λ=460 nm) was recorded using a microplate reader and analyzed to determine the inhibition of HBeAg expression (%) in relation to the negative control (100% expression). The inhibitory activity (%) of compounds 1 and 2 in comparison to LAM (positive control) was presented.

Structure-based in silico molecular docking analysis. The structure-based interactions of HBV proteins (wt-POL 'YMDD' and mut-POL 'YIDD') with the anti-HBV active compounds 1 and 2 and the standard LAM were analyzed by molecular docking in AutoDock 4.2 (20). Previously, the 3D structures of HBV wt-POL and mut-POL were modelled using HIV-polymerase/reverse transcriptase (protein data bank ID: 1RTD) as template (16,20). The modeled proteins (targets) were prepared by deleting water molecules or any attached hetero atoms, and by adding hydrogens. Kollman charges were assigned and the protein structures were energy-minimized using the Merck molecular force field, as described previously (20). The 2D structures of the test ligands [ACT and alkaloid acetyl-β-carboline (ABC)] and the control ligand (LAM) were drawn in ChemDraw Pro 8.0 (PerkinElmer, Inc.), which were then prepared for docking by assigning bond orders and angles, and by defining Gasteiger partial charges. Furthermore, the ligands were energy-minimized by Universal force field, as described previously (20).

Docking was performed inside a defined grid box in the protein structure, which includes the key amino acid residues in the active-site/binding-motif. For wt-POL catalytic residues (Tyr, Met, Asp, and Asp of 'YMDD' motif) and mut-POL residues (Tyr, Ile, Asp, and Asp of 'YIDD' motif), dimensions of the grid boxes were adjusted to 28x28x28 Å and centered at 47x31x35 Å, with 0.375 Å spacing. The Lamarck genetic algorithm was employed for the global search, whereas the Solis-Wets method was used for the local search, as previously described (16,20). A total of $2.5x10^6$ energy calculations was computed for each run, where a total of 10 docking runs were performed. The following conditions were set: Population size, 150; translational step, 0.2; quaternions, 5; and torsions, 5. The van der Waals' and electrostatic parameters were also calculated with using the distance-dependent dielectric function. The docking affinity (K_d) of each ligand for the protein targets was estimated from its docking energy (ΔG) using the following formula: $\Delta G=-2.303RT \log_{10}K_d$, where R (1.987 cal/mol) was the universal gas constant and T (298 K) was the temperature (28).

Statistical analysis. All data of the analyzed samples were presented as the mean ± SEM of three determinants (i.e., values of triplicated samples). In a set of data, total variation was determined by performing one-way analysis of variance (ANOVA), followed by Dunnett's test (Excel 2010; Microsoft Corporation). $P<0.05$ was considered to indicate a statistically significant difference.

Results

Isolation of bioactive compounds from R. stricta. In total, two known compounds 1 and 2 isolated from the EtOAc-fraction of the aerial parts of *R. stricta* were identified after comparing their physical and spectral data available in the literature (23-25).

Compound 1 was a yellow, needle-like crystallized substance in MeOH that was soluble in DMSO, with the general chemical formula of $C_{16}H_{12}O_5$. ESI-HRMS: m/z 285.12 $(M+H)^+$. Its ^{1}H-NMR (DMSO-d_6, 700 MHz) δ are as follows: 12.82 (1H, s, 5-OH), 9.76 (1H,br s, 7-OH), 7.94 (2H, d, J=9.0 Hz, H-2',6'), 7.09 (2H, d, J=8.8 Hz, H-3',5'), 5.98 (1H, s, H-3), 5.41 (1H, d, J=1.8 Hz, H-8) and 5.19 (1H, d, H-3, J=2.4 Hz, H-6). Its ^{13}C-NMR (DMSO-d6, 125 MHz) δ were as follows: 182.6 (C-4), 165.1 (C-7), 164.2 (C-2), 163.2 (C-4'), 162.3 (C-5), 156.2 (C-9), 127.2 (C2',6'), 121.6 (C-1'), 115.3 (C-3',5'), 102.9 (C-10), 102.6 (C-3), 98.6 (C-6) and 92.0 (C-8). Based on the available structural data (23,24), it was identified as ACT, a flavonoid (Fig. 1A).

Compound 2 was a yellow amorphous solid substance that was also soluble in DMSO, with the general chemical formula of $C_{12}H_{10}N_2$. ESI-HRMS: m/z 183.3 $(M+H)^+$. Its ^{1}H-NMR (DMSO-d_6, 700 MHz) δ are as follows: 8.13 (1H, d, 5.3 Hz, H-3), 6.98 (1H, d, 5.6 Hz, H-4), 7.98 (1H, d, 8.0 Hz, H-5), 6.92 (1H, t, 6.8 Hz, H-6), 7.45 (1H, t, 7.2 Hz, H-7), 7.65 (1H, d, 8.0 Hz, H-8), 10.65 (1H, s, br, H-10) and 2.79 (3H, s, CH_3). It ^{13}CNMR (DMSO-d6, 125 MHz) δ were as follows: 143.0 (C-1),

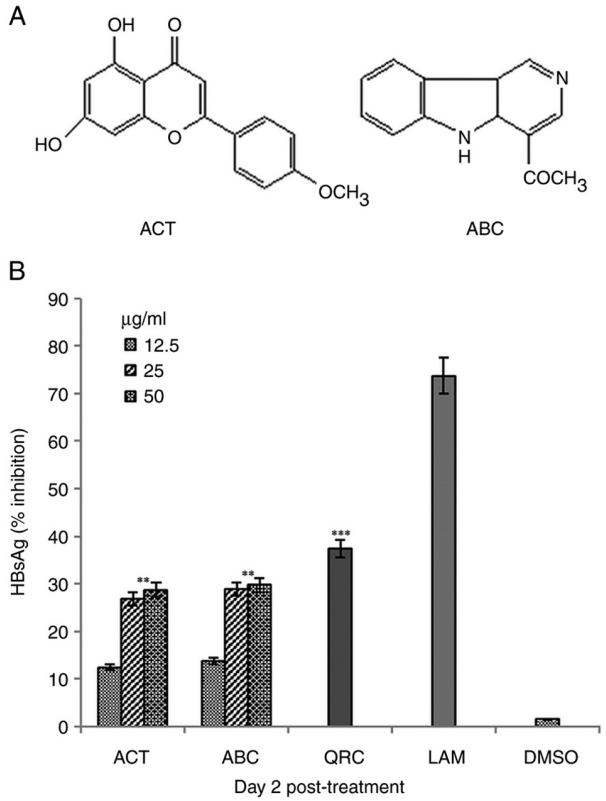

Figure 1. Effects of ACT and ABC on HBsAg production in HepG2.2.15 cells. (A) Structures of *Rhazya stricta*-derived ACT and ABC. (B) Dose-dependent (12.5, 25 and 50 μM) inhibition of HBsAg in HepG2.2.15 cells at day 2 (a single time-point) post-treatment. QRC (12.5 μg/ml) and LAM (2 μM) served as positive controls whilst DMSO (0.1%) acted as a negative control. Data are presented as the mean ± mean ± standard error of three determinants (triplicated values of each sample). **P<0.01 and ***P<0.001 vs. LAM (day 2). ACT, acacetin; ABC, 1-acetyl-β-carboline; HBsAg, HBV surface antigen; QRC, quercetin; LAM, lamivudine.

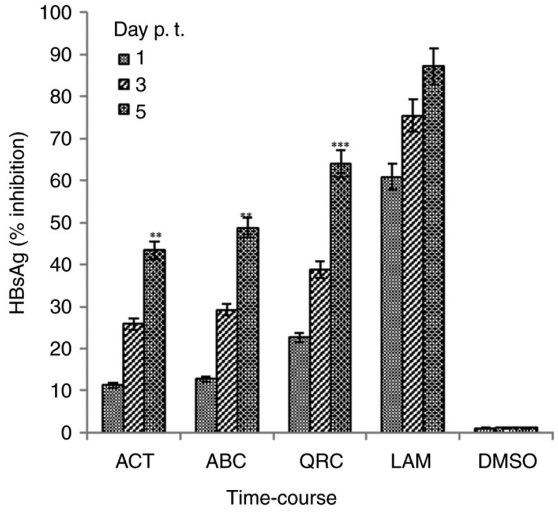

Figure 2. Time-course inhibition of HBsAg by *Rhazya stricta*-derived ACT and ABC at the optimal selected dose (25 μg/ml, each) at day 1, 3 and 5 post-treatment in HepG2.2.15 cells. QRC (12.5 μg/ml) and LAM (2 μM) served as positive controls, whilst DMSO (0.1%) acted as a negative control. Data are presented as the mean ± standard error of three determinants (triplicated values of each sample). **P<0.01 and ***P<0.001 vs. LAM (day 3 and 5). ACT, acacetin; ABC, 1-acetyl-β-carboline; HBsAg, HBV surface antigen; QRC, quercetin; LAM, lamivudine; p.t., post-treatment.

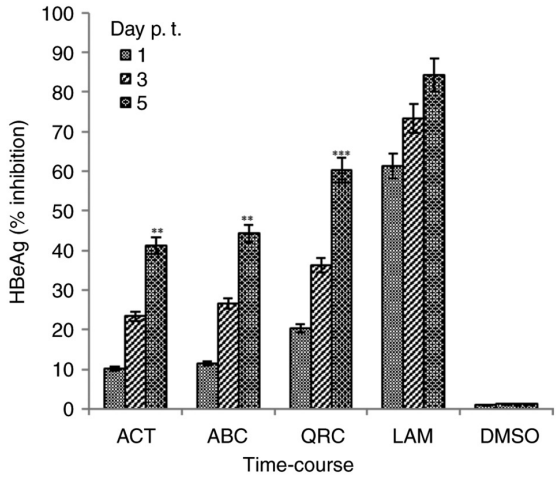

Figure 3. Time-course inhibition of HBeAg by *Rhazya stricta*-derived ACT and ABC at the optimal selected dose (25 μg/ml, each) at day 1, 3 and 5 post-treatment in HepG2.2.15 cells. QRC (12.5 μg/ml) and LAM (2 μM) served as positive controls whilst DMSO (0.1%) acted as a negative control. Data are presented as the mean ± standard error of three determinants (triplicated values of each sample). **P<0.01 and ***P<0.001 vs. LAM (day 3 and 5). HBeAg, hepatitis B e-antigen; ACT, acacetin; ABC, 1-acetyl-β-carboline; QRC, quercetin; LAM, lamivudine; p.t., post-treatment.

138.9 (C-3), 113.2 (C-4), 122.3 (C-5), 120.3 (C-6), 128.6 (C-7), 112.7 (C-8), 135.6 (C-9) and 21.4 (C-11). Based on the structural data (23), it was identified as ABC, an alkaloid (Fig. 1A).

Lack of cytotoxicity exerted by ACT and ABC. Neither of ACT nor ABC tested up to 50 μg/ml showed any sign of toxicity on HepG2.2.15 cells at 72 h, as determined by MTT assay (data not shown). This was in agreement with the observed morphological integrity of the treated cells, when compared with untreated or control cells under the microscope. The CC_{50} value was therefore not determined.

Dose- and time-dependent inhibition of HBsAg synthesis by ACT and ABC. When tested for dose-dependent effects at a single time-point (day 2), ACT and ABC exerted maximal inhibition of HBsAg synthesis at 25 μg/ml, since 50 μg/ml could not significantly potentiate the inhibition of HBsAg any further (Fig. 1B). Therefore, using a single-time point, a single maximal dose of 25 μg/ml was selected for the time-course analysis. Among the three time-points (days 1, 3 and 5), the observed maximal inhibition values of HBsAg production by ACT and ABC were 43.4% (P<0.01 vs. LAM) and 48.7% (P<0.01 vs. LAM) on day 5, respectively. The corresponding value for QRC was 63.9% (P<0.001), compared with that of LAM (87.1%) on day 5 (Fig. 2). Since further culturing with the selected optimal dose resulted in cell over-growth and apoptotic cell death, the assay was not extended beyond day 5.

Downregulation of virus replication by ACT and ABC. Synthesis of HBeAg is a clinical serological marker of active HBV DNA replication (5,26). Therefore, the optimal 25 μg/ml dose was also tested for its effects on HBeAg expression. Among the three time-points tested (days 1, 3 and 5), the

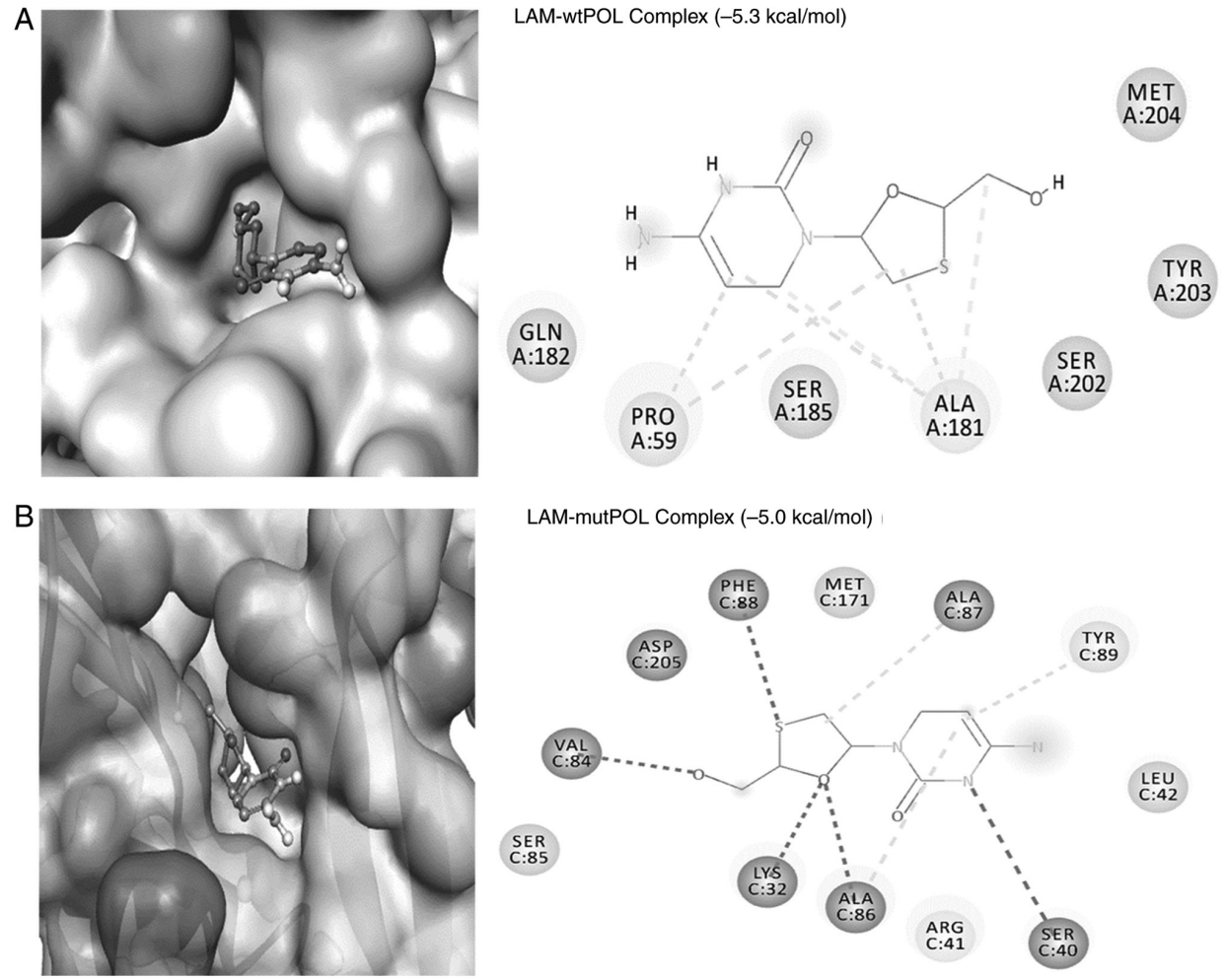

Figure 4. Molecular docking analysis of LAM onto the hepatitis B virus POL protein. Structure-based interaction of LAM (reference drug) with (A) wt-POL ('YMDD' motif's Tyr, Met, Asp and Asp residues) and (B) mut-POL ('YIDD' motif's Tyr, Ile, Asp and Asp residues). LAM, lamivudine; wt-POL, wild-type polymerase; mut-POL, mutant polymerase.

maximal inhibition values of HBeAg synthesis by ACT and ABC were 41.2% (P<0.01 vs. LAM) and 44.2% (P<0.01 vs. LAM) on day 5, respectively. The corresponding value for QRC was 60.2% (P<0.001), compared with that of LAM (84.3%) at day 5 (Fig. 3). Since further culturing with the selected optimal doses led to cell over-growth and apoptotic cell death, the assay was not extended beyond day 5.

Structure-based interactions of the isolated compounds with HBV wt-POL. Molecular docking analysis showed formation of a stable complex between LAM (reference drug) and the HBV wt-POL active-site residues (Fig. 4A). LAM formed two conventional H-bonds with Ala181:O (3.51 Å and 3.66 Å) and four hydrophobic interactions with Pro59 (5.20 Å and 4.42 Å) and Ala181 (5.12 Å and 3.84 Å; Fig. 4A). Notably, in addition to the classical bonding of LAM with the POL 'YMDD (Tyr, Met, Asp, Asp)' motif's residues Tyr203 and Met204, its van der Waals' interactions with Gln182 and Ser185 further strengthened the complex. The binding free energy and the corresponding binding affinity of the LAM-wt-POL complex were estimated to be-5.3 kcal/mol and $7.71x10^3$/M, respectively (Table I).

The flavonoid ACT also formed a stable complex with the target protein wt-POL through hydrogen bonds and hydrophobic interactions (Fig. 5A). The wt-POL residue Lys:HZ1 formed two conventional H-bonds with the O-atom of ACT (2.08 Å and 2.75 Å), whilst Arg41:HH22 interacted with the O-atom of ACT through another conventional H-bond (2.28 Å; Table I). A C-H bond was also formed between ACT and Asp206:OD2 (3.55 Å). In addition, electrostatic (π-anion) interaction with Asp205:OD1 (3.44 Å) and a π-donor hydrogen bond with Ala86:HN (2.86 Å) were also involved in stabilizing the ACT-wt-POL complex. ACT also formed hydrophobic interactions (π-alkyl; 4.78 Å) with Ala86 (Fig. 5A). The ACT-wt-POL complex was further strengthened by van der Waals' interactions with Asp83, Val84, Ser85, Phe88, Tyr89, His160 and Met171. The ACT-wtPOL complex binding energy and docking affinity was estimated to be -6.8 kcal/mol and $1.15x10^5$/M, respectively (Table I).

The alkaloid ABC also formed a stable complex with the target protein wt-POL through two conventional hydrogen bonds involving Lys32:HZ1 and LIG:O (2.20 Å), alongside LIG:HN and Asp205:OD2 (2.04 Å), with a C-H bond between LIG:C and Val84:O (3.59 Å; Table I). In the complex, an electrostatic (π-cation) interaction between Arg41:NH2 and LIG (4.07 Å) was also observed (Table I; Fig. 6A). Furthermore, ABC formed a π-σ hydrophobic interaction with Arg41:CG (3.76 Å) and two

Table I. Molecular docking parameters for the interaction of hepatitis B virus wild-type polymerase ('YMDD' motif) with ACT and ABC.

Interaction between donor and acceptor atoms	Type of interaction	Distance (Å)	Docking energy (ΔG), kcal/mol	Dissociation constant (K_d/mol)
Lamivudine			-5.3	$7.71x10^3$
LIG:C-ALA181:O	Carbon H-bond	3.51		
LIG:C-ALA181:O	Carbon H-bond	3.66		
PRO59-LIG	Hydrophobic (alkyl)	4.42		
PRO59-LIG	Hydrophobic (alkyl)	5.20		
ALA181-LIG	Hydrophobic (alkyl)	5.12		
ALA181-LIG	Hydrophobic (alkyl)	3.84		
ACT			-6.8	$9.72x10^4$
LYS32:HZ1-LIG:O	Conventional H-bond	2.08		
LYS32:HZ1-LIG:O	Conventional H-bond	2.75		
ARG41:HH22-LIG:O	Conventional H-bond	2.28		
LIG:C-ASP206:OD2	Carbon H-bond	3.55		
ASP205:OD1-LIG	Electrostatic (π-anion)	3.44		
ALA86:HN-LIG	H-bond (π-donor)	2.86		
LIG-ALA86	Hydrophobic (π-alkyl)	4.78		
ABC			-6.8	$9.72x10^4$
LYS32:HZ1-LIG:O	Conventional H-bond	2.20		
LIG:HN-ASP205:OD2	Conventional H-bond	2.04		
LIG:C-VAL84:O	Carbon H-bond	3.59		
ARG41:NH2-LIG	Electrostatic (π-cation)	4.07		
ARG41:CG-LIG	Hydrophobic (π-σ)	3.76		
LIG-MET171	Hydrophobic (π-alkyl)	5.05		
LIG-ARG41	Hydrophobic (π-alkyl)	4.97		

ACT, acacetin; ABC, acetyl-β-carboline.

π-alkyl hydrophobic interactions with Met71 (5.05 Å) and Arg41 (4.97 Å; Fig. 6A). The residue Ser85 was found to be involved in an unfavorable acceptor-acceptor interaction with the O-atom of ABC. Additionally, the van der Waals' interactions were also established by the wt-POL residues Ser40, Leu42, Asp83, Val84, Aal87, Phe88, Tyr89 and His160. The docking free energy and binding affinity of the ABC-wt-POL complex were estimated to be -6.8 kcal/mol and $1.15x10^5$/M, respectively (Table I).

Structure-based interactions of the isolated compounds with HBV mut-POL. In the case of mut-POL, LAM was found to form weak interactions with the active-site (Fig. 4B). LAM interacted through four H-bonds with Lys32:HZ1 (2.60 Å), Ser40:O (2.27 Å), Val84:O (1.91 Å) and Ala86:HN (2.94 Å). It also formed a π-Sigma bond with Phe88 (5.45 Å) and three hydrophobic interactions with Ala86 (4.54 Å), Ala87 (5.06 Å) and Tyr89 (4.85 Å; Fig. 4B). Specifically, LAM formed van der Waals' interactions with the 'Tyr-Ile-Asp-Asp' motif's Asp205, as well as residues Arg41, Leu42, Ser85 and Met171. In addition, the binding free energy and binding affinity of LAM-mut-POL complex were calculated as -5.0 kcal/mol and $4.65x10^3$/M, respectively (Table II).

The interaction between ACT and the target protein mut-POL was favored by two H-bonds with Ala86:HN (2.05 and 2.30 Å), two π-cation electrostatic interactions with Lys32:NZ (3.89 Å) and Arg41:NH2 (4.34 Å), in addition to two π-anion electrostatic interactions with Asp83:OD1 (3.41 and 4.13 Å) and Asp205:OD1 (3.29 Å; Fig. 5B). Notably, ACT formed a hydrophobic interaction with Ile204 (5.42 Å) and van der Waals' interactions with Tyr203 and Asp206 of the 'Tyr-Ile-Asp-Asp' motif. The complex was further strengthened by van der Waals' interactions involving with Asn36, Val84, Ser85 and Ala87. The estimated binding free energy and binding affinity of the ACT-mut-POL complex were -6.2 kcal/mol and $3.53x10^4$/M, respectively (Table II).

Docking analysis of ABC and the target protein mut-POL revealed that the complex was mainly stabilized by H-bonds and hydrophobic interactions (Table II). Notably, the NH-group of Ile204 in the 'Tyr-Ile-Asp-Asp' motif formed a H-O bond with ABC (1.85 Å). Similarly, N-atoms of ABC formed two H-bonds with the O-atom of Ser202 (3.01 Å) preceding Tyr203 and the O-atom of Val63 (2.87 Å; Fig. 6B). Furthermore, ABC formed a π-σ and a π-alkyl hydrophobic interaction with Tyr203 and Leu66 residues, respectively. In addition, van der Waals' interactions were also formed with Pro64, Asn65, Ser68 and Ala181 residues in the complex. The estimated docking free energy and binding affinity of ABC-mutPOL complex were -6.0 kcal/mol and $2.52x10^4$/M, respectively (Table II).

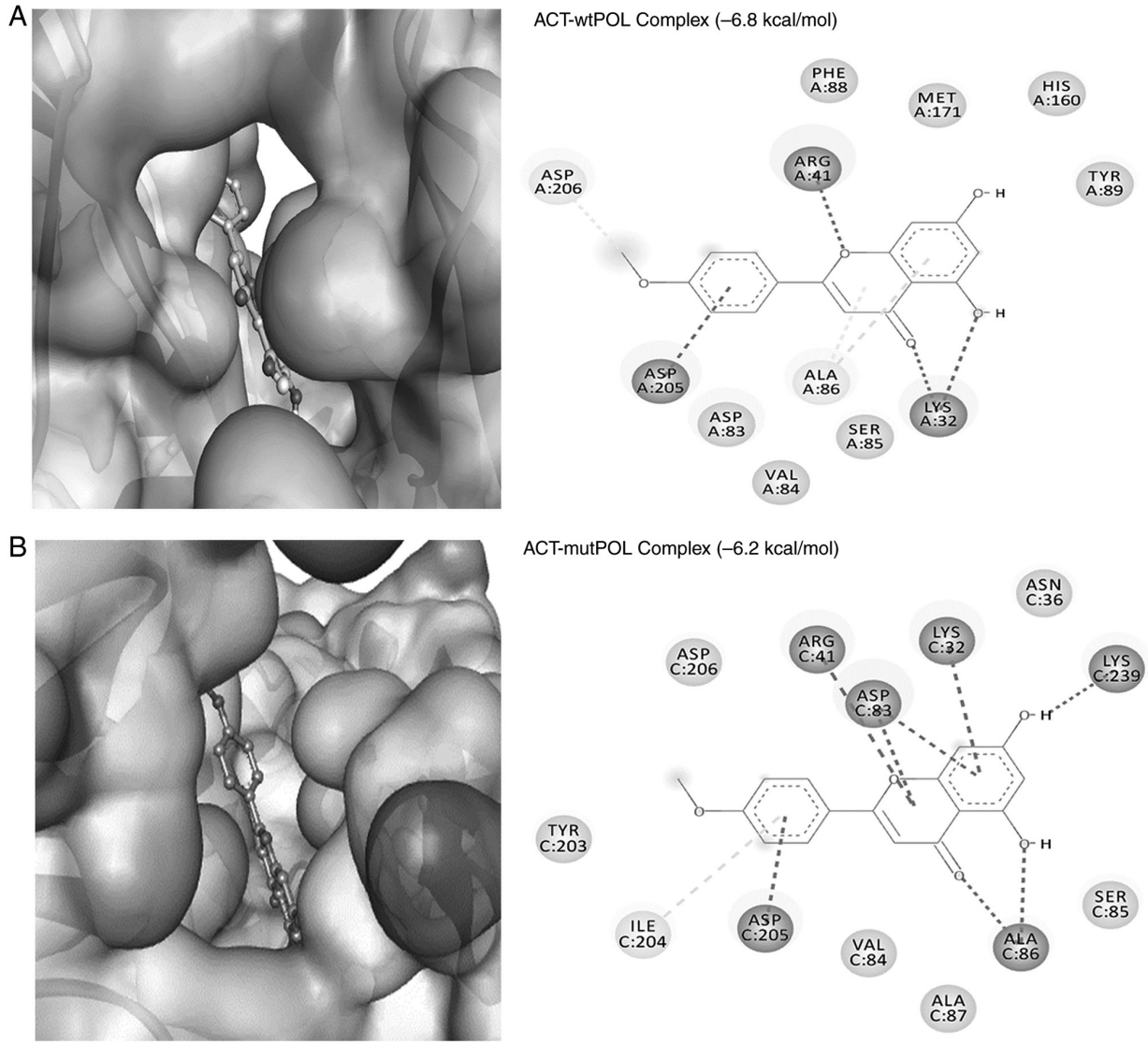

Figure 5. Molecular docking analysis of ACT onto the hepatitis B virus POL protein. Structure-based interaction of ACT with (A) wt-POL ('YMDD' motif's Tyr, Met, Asp and Asp residues) and, (B) mut-POL ('YIDD' motif's Tyr, Ile, Asp and Asp residues). ACT, acacetin; wt-POL, wild-type polymerase; mut-POL, mutant polymerase.

Discussion

Among the known classes of phytochemicals with antiviral potential (2,3), flavonoids are particular noted for their significantly higher activities against several viruses (29,30), including HBV (19-21,27,31,32). Organ or liver toxicity is known to be caused by some antiviral herbal products, notably the Chinese traditional medicines (33). To minimize this risk, the *R. stricta*-derived ACT and ABC were first tested for potential hepatotoxicity in cultured HepG2.2.15 cells. Both compounds were not found to be cytotoxic up to the tested maximal concentration of 50 μg/ml. Therefore, they were then assessed for their anti-HBV efficacies. Notably, due to the close similarity of the genome replication mechanism used by HBV with that of HSV and HIV, the majority of the anti-HSV/HIV drugs are also viable against HBV (26). ACT (100 μg/ml) isolated from *Scoparia dulcis* has been previously reported to inhibit HSV in cultured Vero cells (34). In addition, ACT has been demonstrated to suppress HIV gene expression *in vitro* (35). Consistent with this finding, to the best of our knowledge, the present study reported for the first time the anti-HBV activity of *R. stricta*-derived ACT in cultured HepG2.2.15 cells. ACT (25 μg/ml) maximally inhibited the production of HBsAg by 43.4% and HBeAg by 41.2% compared with those in the untreated control. Comparatively, the standards LAM and QRC suppressed synthesis of HBsAg by 87.1 and 63.9%, respectively, and HBeAg by 84.3 and 64.2%, respectively. Notably, the concentration used to maximally inhibit HBV was 25% less of that used against HSV elsewhere (34).

β-carboline alkaloids are natural compounds with documented antiviral activities (22). Previously, anti-HSV active β-carboline compounds eudistomin C and E have been isolated from the Caribbean tunicate (36-38). Caribbean deep-sea sponge-derived imidazole alkloids topsentin and bromotopsentin have also demonstrated bioactivities against HSV and the human coronavirus A59 (HCoV-A59), whereas dihydrodeoxybromotopsentin was shown to confer activity against HCoV-A59 only (39). In addition, β-carboline alkaloids, such

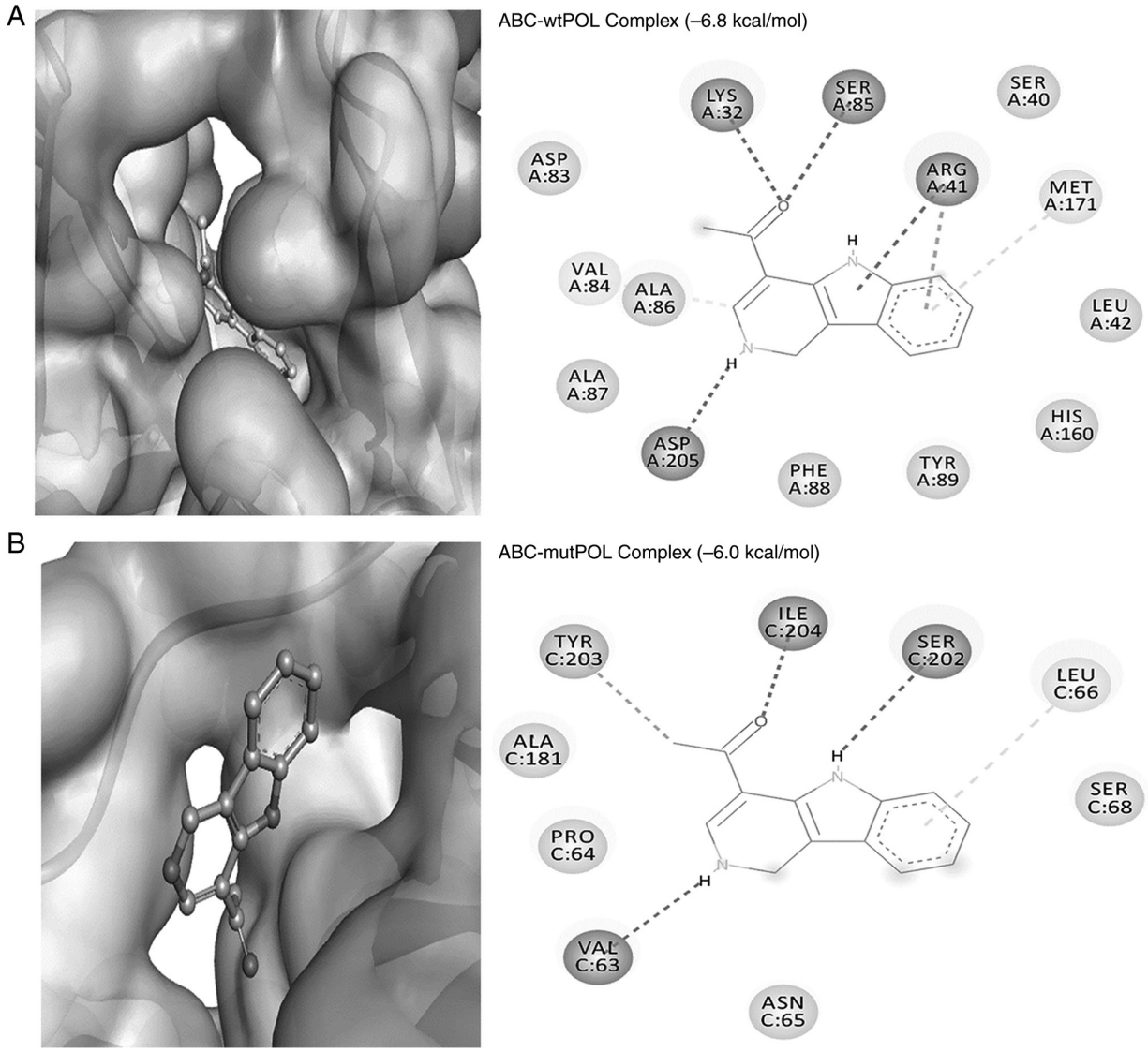

Figure 6. Molecular docking analysis of ABC onto the hepatitis B virus POL protein. (A) Structure-based interaction of ABC with (A) wt-POL ('YMDD' motif's Tyr, Met, Asp, and Asp residues) and, (B) mut-POL ('YIDD' motif's Tyr, Ile, Asp, and Asp residues). ABC, acetyl-β-carboline; wt-POL, wild-type polymerase; mut-POL, mutant polymerase.

as dercitin, from other marine sources, were found to have both anti-HSV and anti-HIV properties (40). Acarnidines, polyandrocarpidines and didemnins were reported to be active against HSV, coxackie virus, equine rhinovirus, paraINV, Rift Valley fever virus, Venezuelan equine encephalomyelitis virus and yellow fever virus (41). Consistent with these observation, a recent study has shown the anti-HBV efficacy of solanopubamine (β-amino-5,22,25-solanidan-23-ol), a steroidal alkaloid isolated from *Solanum schimperianum* (20). In the present study, to the best of our knowledge, the anti-HBV activity of ABC in HepG2.2.15 cells was found for the first time. ABC (25 μg/ml) maximally inhibited the production of HBsAg by 48.7% and HBeAg by 44.2% compared with those in the untreated control. Notably, in a previous study, LAM and QRC have been tested for non-cytotoxicity and their doses were optimized, following which a gene reporter assay was also conducted to confirm their lack of direct or indirect interference with host proteins involved in the production of viral HBsAg and HBeAg (16,17,26).

LAM, the cytidine analog (2',3'-dideoxy-3'-thiacytidine) and other such nucleotide analogs are approved anti-viral drugs for effectively treating chronic hepatitis B (4). The HBV POL catalyzes its DNA replication, where the conserved POL residues Tyr, Met, Asp, and Asp of the 'YMDD' motif incorporates new nucleot(s)ides into its growing single-strand DNA (5). Incorporation of LAM blocks the addition of new nucleosides, resulting in the termination of DNA strand elongation (5). In patients with chronic HBV on long-term LAM therapy, HBV resistance to LAM emerges due to the substitutions of Met to Ile or Val in the 'YMDD' motif. This 'YMDD' to 'YI/VDD' change significantly affects the tertiary structure and hence, the activity of POL (5), leading to inefficient or no incorporation of LAM into the DNA strand, allowing the elongation of the DNA strand and viral replication (5). Molecular docking analyses of the tested anti-HBV active compounds have demonstrated formations of stable complexes with HBV drug-sensitive (wt-POL: 'YMDD') and drug-resistant (mut-POL: 'YIDD') POLs. Both ACT and ABC showed bonding with the catalytic

Table II. Molecular docking parameters for the interaction of hepatitis B virus mutant polymerase ('YIDD' motif) with ACT and ABC.

Interaction between donor and acceptor atoms	Type of interaction	Distance (Å)	Docking energy (ΔG); kcal/mol	Dissociation constant (K_d/mol)
Lamivudine			-5.0	$4.65x10^3$
LYS32:HZ1-LIG:O	Conventional H-bond	2.60		
ALA86:HN-LIG:O	Conventional H-bond	2.94		
LIG:N-SER40:O	Conventional H-bond	2.27		
LIG:O-VAL84:O	Conventional H-bond	1.91		
LIG:S-PHE88	π-sulfur	5.45		
ALA86-LIG	Hydrophobic (alkyl)	4.54		
ALA87-LIG	Hydrophobic (alkyl)	5.06		
TYR89-LIG	Hydrophobic (π-alkyl)	4.85		
ACT			-6.2	$3.53x10^4$
ALA86:HN-LIG:O	Conventional H-bond	2.05		
ALA86:HN-LIG:O	Conventional H-bond	2.30		
LYS32:NZ-LIG	Electrostatic (π-cation)	3.89		
ARG41:NH2-LIG	Electrostatic (π-cation)	4.34		
ASP83:OD1-LIG	Electrostatic (π-anion)	3.41		
ASP83:OD1-LIG	Electrostatic (π-anion)	4.13		
ASP205:OD1-LIG	Electrostatic (π-anion)	3.29		
LIG-ILE204	Hydrophobic (π-alkyl)	5.42		
ABC			-6.0	$2.52x10^4$
ILE204:HN-LIG:O	Conventional H-bond	1.85		
LIG:N-SER202:O	Conventional H-bond	3.01		
LIG:N-VAL63:O	Conventional H-bond	2.87		
LIG:C-TYR203	Hydrophobic (π-σ)	3.99		
LIG-LEU66	Hydrophobic (π-alkyl)	5.25		

ACT, acacetin; ABC, acetyl-β-carboline.

'Tyr-Met/Ile-Asp-Asp' motif residues, including other interactions in their respective complexes. Notably, ACT interacted with wt-POL Asp205 and Asp206, as well as mut-POL Tyr203 and Asp206, whilst ABC interacted with wt-POL Asp205, as well as mutPOL Tyr203 and Ile204. Inhibition of HBV POL activity leads to the downregulation of viral RNA transcription and therefore, translation of its proteins, including HBsAg and HBeAg (5,26). In conclusion, to the best of our knowledge, the present study shows promising *in vitro* anti-HBV efficacies of ACT and ABC, endorsed by *in silico* data, for the first time. However, further molecular and pharmacological studies are required to validate their pre-clinical therapeutic potential.

Acknowledgements

Not applicable.

Funding

The present study was supported by the Researchers Supporting Project (grant no. RSP2023R379), King Saud University, Riyadh, Saudi Arabia.

Availability of data and materials

The datasets used and/or analyzed during the current study are available from the corresponding author on reasonable request.

Authors' contributions

MKP and MSA conceptualized the study, performed *in vitro* assays, collected and analyzed data, and wrote the manuscript. TAA, MA and HMA isolated and characterized the compounds, and contributed to writing. ARA performed the statistical analysis. MTR and MFA performed the *in silico* analysis and contributed to writing. All authors read and approved the final manuscript. MKP and TAA confirm the authenticity of all the raw data.

Ethics approval and consent to participate

Not applicable.

Patient consent for publication

Not applicable.

Competing interests

The authors declare that they have no competing interests.

References

1. Kapoor R, Sharma B and Kanwar SS: Antiviral phytochemicals: An overview. Biochem Physiol 6: 220, 2017.
2. Ben-Shabat S, Yarmolinsky L, Porat D and Dahan A: Antiviral effect of phytochemicals from medicinal plants: Applications and drug delivery strategies. Drug Deliv Transl Res 10: 354-367, 2020.
3. Parvez MK, Arbab AH and Al-Dosari MS: An update on natural or herbal drugs against hepatitis B virus. In: Advances in Medicine and Biology. Berhardt LV (ed). Vol 179. NOVA Science Publishers, Inc., New York, NY, pp159-184, 2021.
4. World Health Organization (WHO). Hepatitis B. WHO, Geneva, 2022. https://www.who.int/news-room/fact-sheets/detail/hepatitis-b.
5. Devi U and Locarnini S: Hepatitis B antivirals and resistance. Curr Opin Virol 3: 495-500, 2013.
6. Marwat SK, Usman K, Shah SS, Anwar N and Ullah I: A review of phytochemistry, bioactivities and ethno medicinal uses of *Rhazya stricta* decsne (apocynaceae). Afr J Microbiol Res 6: 1629-1641, 2012.
7. Gilani SA, Kikuchi A, Khan ZS, Khattak ZI and Watanabe KN: Phytochemical, pharmacological and ethnobotanical studies of *Rhazya stricta* decne. Phytother Res 21: 301-307, 2007.
8. Ali BH, Al-Qarawi AA, Bashir AK and Tanira MO: Phytochemistry, pharmacology and toxicity of *Rhazya stricta* decne: A review. Phytother Res 14: 229-234, 2000.
9. Albeshri A, Baeshen NA, Bouback TA and Aljaddawi AA: A review of *Rhazya stricta* decne phytochemistry, bioactivities, pharmacological activities, toxicity, and folkloric medicinal uses. Plants (Basel) 10: 2508, 2021.
10. Sultana N and Khalid A: Phytochemical and enzyme inhibitory studies on indigenous medicinal plant *Rhazya stricta*. Nat Prod Res 24: 305-314, 2010.
11. Albeshri A, Baeshen NA, Bouback TA and Aljaddawi AA: Evaluation of cytotoxicity and antiviral activity of *Rhazya stricta* decne leaves extract against influenza A/PR/8/34 (H1N1). Saudi J Biol Sci 29: 03375, 2022.
12. Baeshen MN, Attar R, Bouback TA, Albeshri AO, Baeshen NN, Karkashan A, Abbas B, Aljaddawi AA, Almulaikyd YQ, Mahmoude SH, *et al*: Assaying for antiviral activity of the folkloric medicinal desert plant *Rhazya stricta* on coronavirus SARS-CoV-2. Biotech Biotechnol Equip 36: 68-74, 2022.
13. Bukhari NA, Al-Otaibi RA and Ibhrahim MM: Phytochemical and taxonomic evaluation of *Rhazya stricta* in Saudi Arabia. Saudi J Biol Sci 24: 1513-1521, 2017.
14. Lanjwani AH, Ganghro AB and Khuhawar TMJ: Phytochemical analysis and biological activity of different parts of *Rhazya stricta*. Rawal Med J 43: 532-535, 2018.
15. Badshah SL, Faisal S, Muhammad A, Poulson BG, Emwas AH and Jaremko M: Antiviral activities of flavonoids. Biomed Pharmacother 140: 11596, 2021.
16. Parvez MK, Tabish Rehman M, Alam P, Al-Dosari MS, Alqasoumi SI and Alajmi MF: Plant-derived antiviral drugs as novel hepatitis B virus inhibitors: Cell culture and molecular docking study. Saudi Pharm J 27: 89-400, 2019.
17. Parvez MK, Al-Dosari MS, Alam P, Rehman MT, Alajmi MF and Alqahtani AS: The anti-hepatitis B virus therapeutic potential of anthraquinones derived from Aloe vera. Phytother Res 33: 1960-1970, 2019.
18. Parvez MK, Al-Dosari MS, Arbab AH, Al-Rehaily AJ and Abdelwahid MAS: Bioassay-guided isolation of anti-hepatitis B virus flavonoid myricetin-3-O-rhamnoside along with quercetin from Guiera senegalensis leaves. Saudi Pharm J 28: 550-559, 2020.
19. Parvez MK, Ahmed S, Al-Dosari MS, Abdelwahid MAS, Arbab AH, Al-Rehaily AJ and Al-Oqail MM: Novel anti-hepatitis B virus activity of Euphorbia schimperi and its quercetin and kaempferol derivatives. ACS Omega 6: 29100-29110, 2021.
20. Parvez MK, Al-Dosari MS, Rehman MT, Al-Rehaily AJ, Alqahtani AS and Alajmi MF: The anti-hepatitis B virus and anti-hepatotoxic efficacies of solanopubamine, a rare alkaloid from Solanum schimperianum. Saudi Pharm J 30: 359-368, 2022.
21. Wang G, Zhang L and Bonkovsky HL: Chinese medicine for treatment of chronic hepatitis B. Chin J Integr Med 18: 253-255, 2012.
22. Szabó T, Volk B and Milen M: Recent advances in the synthesis of β-carboline alkaloids. Molecules 26: 663, 2021.
23. Qu GR, Liu J, Li XX, Wang SX, Wu LJ and Li X: Flavonoids constituents of Sonchus arvensis L. Zhong Cao Yao 26: 233-235, 1995.
24. Gong FJ, Wang GL and Wang YW: Chemical constituents of the flowers of Dendranthema indicum var. aromaticum. Wuhan Zhiwuxue Yanjiu 23: 610-612, 2005.
25. Cao R, Peng W, Wang Z and Xu A: beta-Carboline alkaloids: Biochemical and pharmacological functions. Curr Med Chem 14: 479-500, 2007.
26. Parvez MK, Sehgal D, Sarin SK, Basir SF and Jameel S: Inhibition of hepatitis B virus DNA replicative intermediate forms by recombinant interferon-gamma. World J Gastroenterol 12: 3006-3014, 2006.
27. Parvez MK, Al-Dosari MS, Basudan OA and Herqash RN: The anti-hepatitis B virus activity of sea buckthorn is attributed to quercetin, kaempferol and isorhamnetin. Biomed Rep 17: 89, 2022.
28. Rehman MT, Ahmed S and Khan AU: Interaction of meropenem with 'N' and 'B' isoforms of human serum albumin: A spectroscopic and molecular docking study. J Biomol Struct Dyn 34: 1849-1864, 2016.
29. Zakaryan H, Arabyan E, Oo A and Zandi K: Flavonoids: Promising natural compounds against viral infections. Arch Virol 162: 2539-2551, 2017.
30. Wang L, Song J, Liu A, Xiao B, Li S, Wen Z, Lu Y and Du G: Research progress of the antiviral bioactivities of natural flavonoids. Nat Prod Bioprospect 10: 271-283, 2020.
31. Ahmed S, Parvez MK, Zia K, Nur-e-Alam M, Ul-Haq Z, Al-Dosari MS and Al-Rehaily AJ: Natural anti-hepatitis B virus flavones isolated from Stachys schimperi Vatke growing in Saudi Arabia. Pharmacog Mag 18: 386-392. 2022.
32. Parvez MK, Al-Dosari MS, Abdelwahid MAS, Alqahtani AS and Alanzi AR: Novel anti-hepatitis B virus-active catechin and epicatechin from Rhus tripartita. Exp Ther Med 23: 398 2022.
33. Parvez MK and Rishi V: Herb-Drug interactions and hepatotoxicity. Curr Drug Metab 20: 275-282, 2019.
34. Singh S, Gupta P, Meena A and Luqman S: Acacetin, a flavone with diverse therapeutic potential in cancer, inflammation, infections and other metabolic disorders. Food Chem Toxicol 145: 111708, 2020.
35. Hayashi K, Hayashl T, Arisawa M and Morita N: Antiviral agents of plant origin. Antiherpetic activity of acacetin. Antiviral Chem Chemother 4: 49-53, 1993.
36. Critchfield JW, Butera ST and Folks TM: Inhibition of HIV activation in latently infected cells by flavonoid compounds. AIDS Res Hum Retroviruses 12: 39-46, 1996.
37. Rinehart KL, Kobayashi J, Harbour GC, Hughes RG Jr, Mizsak SA and Scahill TA: Eudistomins C, E, K, and L, potent antiviral compounds containing a novel oxathiazepine ring from the Caribbean tunicate Eudistoma olivaceum. J Am Chem Soc 106: 1524-1526, 1984.
38. Rinehart KL Jr, Kobayashi J, Harbour GC, Gilmore J, Mascal M, Holt TG, Shield LS and Lafargue F: Eudistomins A-Q, beta-carbolines from the antiviral Caribbean tunicate Eudistoma olivaceum. J Am Chem Soc 109: 3378-3387, 1987.
39. Tsujii S, Rinehart KL, Gunasekera SP, Kashman Y, Cross SS, Lui MS, Pomponi SA and Diaz MC: Topsentin, bromotopsentin, and dihydrodeoxybromotopsentin, antiviral and antitumor bis(indolyl)imidazoles from Caribbean deepsea sponges of the family Halichondriidae. Structural and synthetic studies. J Org Chem 33: 5446-5453, 1998.
40. Gunawardana GP, Kohmoto S, Gunasekera SP, McConnell OJ and Koehn FE: Dercitin, a new biologically active acridine alkaloid from a deep water marine sponge, Dercitus sp. J Am Chem Soc 110: 4856-4858, 1988.
41. Rinehart KL Jr, Gloer JB, Cook JC Jr, Mizsak SA and Scahill TA: Structures of the didemnins, antiviral and cytotoxic depsipeptides from a Caribbean tunicate. J Am Chem Soc 103: 1857-1859, 1981.